Hydrogen Bond Lifetime Dynamics at the Interface of a Surfactant Monolayer

Jnanojjal Chanda and Sanjoy Bandyopadhyay*

Molecular Modeling Laboratory, Department of Chemistry, Indian Institute of Technology, Kharagpur 721302, India

Received: August 11, 2006; In Final Form: September 14, 2006

The dynamics of water near the polar headgroups of surfactants in a monolayer adsorbed at the air/water interface is likely to play a decisive role in determining the physical behavior of such organized assemblies. We have carried out an atomistic molecular dynamics (MD) simulation of a monolayer of the anionic surfactant sodium bis(2-ethyl-1-hexyl) sulfosuccinate (aerosol-OT or AOT) adsorbed at the air/water interface. The simulation is performed at room temperature with a surface coverage of that at the critical micelle concentration (78 Å^2/molecule). Detailed analyses of the lifetime dynamics of surfactant−water (SW) and water−water (WW) hydrogen bonds at the interface have been carried out. The nonexponential hydrogen bond lifetime correlation functions have been analyzed by using the formalism of Luzar and Chandler, which allowed identification of the bound states at the interface and quantification of the dynamic equilibrium between bound and quasi-free water molecules, in terms of time-dependent relaxation rates. It is observed that the water molecules present in the first hydration layer form strong hydrogen bonds with the surfactant headgroups and hence have longer lifetimes. Importantly, it is found that the overall relaxation of the SW hydrogen bonds is faster for those water molecules which form two hydrogen bonds with the surfactant headgroups than those forming one such hydrogen bond. Equally interestingly, it is further noticed that water molecules beyond the first hydration layer form weaker hydrogen bonds than pure bulk water.

1. Introduction

The formation and breaking of hydrogen bonds in liquid water is responsible for many of its exotic structural and dynamical properties.[1−9] Molecular dynamics (MD) simulations can provide direct quantitative information on the dynamics of hydrogen bonds by calculating different hydrogen bond time correlation functions, as proposed first by Stillinger[3] and developed further by Luzar and Chandler.[4,5] The simulation studies in general have shown that the relaxation behavior of hydrogen bonds in liquid water is nonexponential in nature. Luzar and Chandler[4,5] have proposed a simple model to describe the kinetics of hydrogen bonds in water. The model treats the hydrogen bond dynamics as an activated process, where the rate of relaxation is characterized by a reactive flux correlation function formalism. These studies revealed that the nonexponential relaxation behavior at long times arises due to the coupling of hydrogen bond dynamics and the diffusional motion of water.[4]

It is known that the regular hydrogen bond network in pure water gets disrupted in aqueous solutions containing hydrogen bonding solutes. Chandra and co-workers[10] have extensively studied the properties of hydrogen bonds of aqueous electrolyte solutions. Importantly, they have shown that the hydrogen bond relaxation in aqueous alkali halide solutions slows with increasing ion concentration. The properties of water hydrogen bonds in a restricted environment, such as at an interface, are also greatly different than those in pure water.[11−22] Berne and co-workers[11] have shown that the dynamics of hydrogen bonds at the air/water interface is faster than that in pure bulk water. Recently, the properties of hydrogen bonds at the interface between water and organic liquids have been studied.[12] It is shown that the hydrogen bond dynamics in such systems depend strongly on the nature of the organic liquids. It is known that the polar headgroups of surfactants in an aqueous micellar solution interact strongly with the hydration layer water molecules. Balasubramanian and co-workers[13−15] have recently studied the structure, energetics, and dynamics of hydrogen bonds formed near the surface of an anionic micelle, cesium pentafluorooctanoate (CsPFO). They have shown that the lifetimes of the hydrogen bonds between the polar headgroups of surfactants and water are much longer than the lifetimes of hydrogen bonds between water molecules themselves. Recently, Bruce et al.[16] have shown that the water molecules near the surface of a sodium dodecyl sulfate (SDS) micelle form a distorted network of hydrogen bonds among themselves. Faeder and Ladanyi[17] have studied the characteristics of hydrogen bonds in the interior of reverse micelles and the corresponding influence on the dynamics and structure of the interfacial water.

There are several reports on the study of the microscopic properties of surfactant assemblies adsorbed at different interfaces using simulation methods.[23−34] In an early work, Tarek et al.[23] reported MD studies of the cationic surfactant cetyltrimethylammonium bromide (CTAB) adsorbed at the air/water interface at different concentrations. Their results were in good agreement with experimental data. Self-assembly of nonionic surfactants at a hydrophilic surface has been studied by Wijmans and Linse[24] using Monte Carlo methods. Kuhn and Rehage[25−27] have studied the orientation and dynamic properties of monododecyl pentaethylene glycol ($C_{12}E_5$) monolayers adsorbed at air/water and oil/water interfaces. Recently, water penetration in different surfactant monolayers at the CO_2/water interface has been studied by Rossky and co-workers.[29] Smit and co-workers[30,31] have employed dissipative particle dynamics simulations to investigate the effect of surfactant structure on the

* To whom correspondence should be addressed. E-mail: sanjoy@chem.iitkgp.ernet.in. Phone: 91-3222-283344. Fax: 91-3222-255303.

10.1021/jp065203+ CCC: $33.50
Published on Web 10/24/2006

bending moduli of the adsorbed monolayers. We have recently studied in great detail the microscopic properties of both ionic as well as nonionic surfactant monolayers adsorbed at the air/water interface.[32−34] Our studies revealed that the interfacial water molecules have a strong influence on the orientational and other properties of the surfactant molecules.

Although there are reports (as discussed above) on the study of hydrogen bond dynamics in aqueous micellar solutions,[13−16] not much attempt has been made to study the microscopic details of the dynamics of hydrogen bonds at the interface of a flat surfactant monolayer in contact with water. Eisenthal and co-workers[35] have used time-resolved second harmonic generation spectroscopy to study the solvation dynamics at the air/water interface with and without the presence of surfactant films. They have shown that the rearrangement of the network of hydrogen bonds at the interface due to the presence of the surfactant molecules is characterized by different librational, orientational, and translational motions of water molecules. Using MD simulations, Laria and co-workers[36] have shown that, in addition to the effect of rearrangement of the hydrogen bond network, the solvation dynamics at the air/water interface containing a surfactant film is also correlated with the spatial domains of the surfactants.

In this article, we report the microscopic details of the hydrogen bond lifetime dynamics at the interface of an adsorbed surfactant monolayer. In particular, we have chosen an anionic surfactant monolayer, comprised of sodium bis(2-ethyl-1-hexyl) sulfosuccinate ($(C_8H_{17}OOC)_2C_2H_3SO_3^-\ Na^+$) molecules, commonly known as aerosol-OT or AOT. AOT and its analogues represent an important class of commercial surfactants which contain small branched double tails.[33] The rest of the article is organized as follows. In the next section, we discuss the setup of the simulation system and a brief description of the methodologies employed. The results obtained from our investigations are presented and discussed in the following section. In the last section, we summarize the important findings and the conclusions reached from our study.

2. System Setup and Simulation Details

The initial configuration of the constant temperature and volume (NVT) simulation system was set up by arranging a uniform monolayer of 32 surfactants with the headgroup sulfur atoms on an appropriate 4×4 body-centered square lattice in the *xy* plane with the hydrocarbon chains extending away from the lattice plane. The lattice constants were chosen to give a surface area per molecule of 78 Å^2, corresponding to the experimentally determined value for adsorption at the air/water interface at the critical micelle concentration (cmc).[37] Then, two such Langmuir type monolayers with their headgroups solvated were placed on two opposite sides of a roughly 30 Å thick slab of water molecules. The necessary reasons for choosing such an arrangement have been discussed in our earlier work.[33] Sixty-four sodium counterions were then placed in the aqueous layer by randomly replacing 64 water molecules. The simulation system contained 64 surfactant chains, 2025 water molecules, and 64 sodium counterions. The dimensions of the simulation box in the *x* and *y* direction were 50 Å, while the *z* dimension was kept large at ∼150 Å.

The simulations utilized the Nosé−Hoover chain thermostat extended system method[38] as implemented in the PINY-MD computational package.[39] A recently developed reversible multiple time step algorithm, RESPA,[38] allowed us to employ a 4.5 fs MD time step. Electrostatic interactions were calculated by using the particle mesh Ewald (PME) method.[40] The PME and RESPA were combined following the method suggested by Marchi and co-workers.[41,42] The minimum image convention[43] was employed to calculate the Lennard-Jones interactions and the real-space part of the Ewald sum using a spherical truncation of 7 and 10 Å, respectively, for the short and long range parts of the force decomposition. The simulation system was first equilibrated at constant temperature ($T = 298$ K) and volume (NVT) for about 2 ns. This was then followed by an NVT production run of approximately 4 ns duration, during which the trajectory was stored with a time resolution of 450 fs for subsequent analysis. To investigate the ultrafast properties, a section of the equilibrium trajectory was also stored at a higher time resolution of 18 fs. The CHARMM27 all-atom force field and potential parameters for lipids[44] were employed to describe the interaction between the surfactant molecules, while the TIP3P model,[45] which is consistent with the chosen surfactant force field, was employed for modeling water.

3. Results and Discussion

The perturbation of regular structural and dynamical properties of water constrained at the interface of a monolayer of charged surfactants such as AOT is expected to be correlated with the network of hydrogen bonds formed between water and the surfactant headgroups. An investigation of the microscopic mechanism of the formation and breaking of hydrogen bonds between interfacial water molecules and the surfactant headgroups is therefore crucial to understand the overall behavior of surfactant aggregates at an interface.

3.1. Definition of Interfacial Water and Hydrogen Bonds. We have divided the interfacial aqueous layer into three regions. Those water molecules which are within 5 Å from the sulfur atoms of the surfactant headgroups are said to be in region 1. These are hydration layer water molecules and essentially present within the first coordination shell of the sulfur atoms.[33] Region 2 is comprised of those water molecules which are within 5−8 Å from the sulfur atoms, while those beyond 8 Å are said to be in region 3. The distances are measured with respect to both of the monolayers by tagging the water molecules along the simulated trajectory.

Generally, either a geometric[4,46,47] or an energetic[45,48−50] criterion is used to define a hydrogen bond between a pair of water molecules. In this work, we have employed the latter criterion to define water−water (WW) hydrogen bonds. According to this definition, a WW hydrogen bond is said to exist if the distance between the two oxygen atoms of the tagged pair of water molecules is within 3.5 Å, and if the pair energy is less than −2.5 kcal/mol.[48,50,51]

We have also employed an energetic criterion to define a surfactant−water (SW) hydrogen bond. Such hydrogen bonds are formed between the oxygen atoms of the sulfonate headgroups of the surfactants and the interfacial water molecules. To define the energy cutoff necessary to set such a criterion, we have evaluated the distribution of the pairwise interaction energy between the sulfonate headgroups and the water molecules whose oxygen atoms are within a distance of 3.5 Å from at least one oxygen atom of the sulfonate group of any surfactant molecule. The distribution is shown in Figure 1. The corresponding distribution for the water−water pairwise interaction energy in bulk water is also displayed for comparison. The data for bulk water are obtained from a MD simulation of pure TIP3P water at room temperature and agree well with earlier reports.[14,45] For the headgroup−water pair energy distribution, a tall peak near zero energy arises from pairs which are separated by large distances. The distinct peak at around −9 kcal/mol

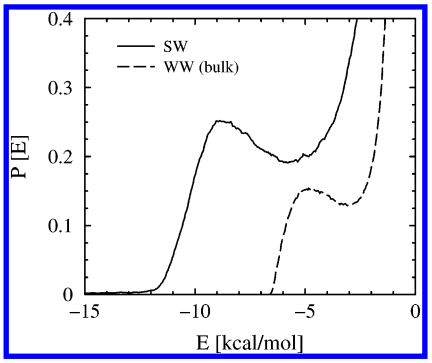

Figure 1. Potential energy distributions of surfactant headgroups and the interfacial water molecules whose oxygen atoms are within 3.5 Å from at least one of the oxygen atoms of the surfactant headgroups (solid line). A corresponding distribution for pairs of water molecules in the bulk is also shown (dashed line).

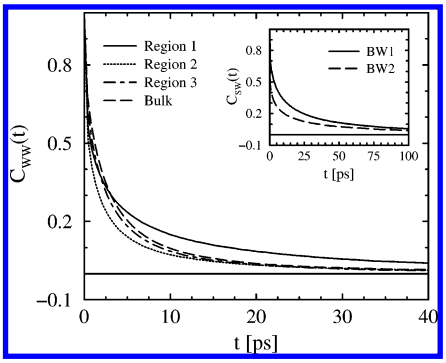

Figure 2. Intermittent hydrogen bond time correlation function, $C_{WW}(t)$, for the hydrogen bonds formed between the water molecules in three regions of the aqueous layer as well as that for pure bulk TIP3P water. Region 1 comprises water molecules that are within 5 Å from the headgroup sulfur atoms; those that are within 5−8 Å are in region 2, and those that are beyond 8 Å are said to be in region 3. The inset shows the corresponding function, $C_{SW}(t)$, for BW1 and BW2 types of water molecules present in the first hydration layer (region 1).

corresponds to a hydrogen bonded pair. The minimum in the distribution obtained at around −5 kcal/mol is chosen to define the energy cutoff for SW hydrogen bonds. Thus, in this work, a SW hydrogen bond is considered to be formed if (i) the oxygen atom of the water is within 5 Å from the sulfur atom of the sulfonate headgroup, (ii) the oxygen atoms of the water and the sulfonate group are within 3.5 Å, and (iii) the pairwise interaction energy between the water and the sulfonate group of the surfactant is less than −5 kcal/mol. Similar energetic criteria have recently been used to define hydrogen bonds in aqueous micellar solution.[14,15] Recently, Pal et al.[14] have classified the water present in the hydration layer of a micellar solution of cesium pentafluorooctanoate (CsPFO) in three categories, depending on whether they form zero, one, or two hydrogen bonds with the surfactants. Adopting their formalism, we have subdivided the first hydration layer water molecules of the AOT monolayer into three types, BW1, BW2, and FW. A BW1 water molecule is that which is bound to a sulfonate headgroup by a single hydrogen bond, while a BW2 water molecule forms two hydrogen bonds with two different sulfonate groups. There is another type of water molecules which are present in the hydration layer but are not bound to any headgroup. Those are free water molecules and are denoted as FW.

Applying the hydrogen bonding criteria as discussed above, we find the ratio FW/BW1/BW2 to be 34:52:14. It is expected that, due to the dynamic nature of the monolayer interface, there will be a continuous exchange of water molecules among the three types as well as with bulk water. However, such an exchange process has not been studied in the present work. Next, we study in detail the dynamics of SW hydrogen bonds and the influence of the monolayer on the WW hydrogen bonds as a function of distance from the surfactant headgroups.

3.2. Hydrogen Bond Lifetimes. The dynamics of WW and SW hydrogen bonds have been characterized in terms of two time correlation functions (TCFs), namely, the continuous hydrogen bond time correlation function, $S(t)$, and the intermittent hydrogen bond time correlation function, $C(t)$.[3,50] These TCFs are defined as

$$S(t) = \frac{\langle h(0)\cdot H(t)\rangle}{\langle h\rangle} \tag{1}$$

and

$$C(t) = \frac{\langle h(0)\cdot h(t)\rangle}{\langle h\rangle} \tag{2}$$

These definitions are based on two hydrogen bond population variables, $h(t)$ and $H(t)$. The variable $h(t)$ is unity when a particular pair of sites (SW or WW) is hydrogen bonded at time t according to the definition used and zero otherwise. The variable $H(t)$, on the other hand, is defined as unity, when the tagged pair of sites remain continuously hydrogen bonded from time $t = 0$ to time t, and zero otherwise. Thus, $S(t)$ describes the probability that a hydrogen bond formed between two sites at time zero remains bonded at all times up to t. In other words, $S(t)$ provides a strict definition of the lifetime of a tagged hydrogen bond. The correlation function, $C(t)$, on the other hand, describes the probability that a particular tagged hydrogen bond is intact at time t, given it was intact at time zero. Thus, $C(t)$ is independent of possible breaking of hydrogen bonds at intermediate times and allows reformation of broken bonds. In other words, it allows recrossing the barrier separating the bonded and nonbonded states, as well as the long time diffusive behavior. Therefore, the relaxation of $C(t)$ provides information about the structural relaxation of a particular hydrogen bond.

We have calculated the time correlation functions, $C_{WW}(t)$ for WW and $C_{SW}(t)$ for SW hydrogen bonds. The function $C_{WW}(t)$ is calculated by averaging over different time origins for the water molecules present in the three hydration layers or regions (defined earlier), which are displayed in Figure 2. For comparison, the corresponding relaxation behavior for pure bulk TIP3P water is also shown. The SW hydrogen bond correlation function, $C_{SW}(t)$, is calculated separately for BW1 and BW2 types of water molecules, as shown in the inset of Figure 2. It is apparent from the figure that the structural relaxation of the SW hydrogen bonds is much slower than that for the WW hydrogen bonds in bulk water as well as that for water in the three regions at the monolayer interface. Such slow relaxation behavior has been observed earlier for hydrogen bonds formed at the surface of surfactant micelles[13,15] as well as at the interface of phospholipid bilayers.[52] This arises due to strong interaction between the polar headgroups and the hydration layer water molecules in such amphiphilic molecular aggregates. Interestingly, we note that the function $C_{SW}(t)$ relaxes faster for the hydrogen bonds formed by BW2 type water molecules than that formed by BW1 type. The calculated average energy of a SW hydrogen bond formed by a BW1 water is found to be −8.9 kcal/mol, while that formed by a BW2 water is −8.3 kcal/mol. Thus, on average, a hydrogen bond formed by BW2 water with a surfactant headgroup is weaker. This is an important observation which suggests that the BW2 water molecules are in a

TABLE 1: Multiexponential Fitting Parameters for the Surfactant−Water (SW), $C_{SW}(t)$, and Water−Water (WW), $C_{WW}(t)$, Intermittent Hydrogen Bond Time Correlation Functions (Corresponding Parameters for Bulk TIP3P Water Are Also Listed for Comparison; $\langle\tau_c\rangle$ is the Average Time Constant)

surfactant−water (SW)				water−water (WW)			
type	time constant (ps)	amplitude (%)	$\langle\tau_c\rangle$ (ps)	region	time constant (ps)	amplitude (%)	$\langle\tau_c\rangle$ (ps)
BW1	0.38	36.2	19.94	region 1	0.24	46.3	5.46
	8.96	39.6			3.32	34.8	
	67.16	24.2			22.17	18.9	
BW2	0.23	58.0	13.26	region 2	0.24	49.9	2.22
	7.39	25.8			2.13	41.4	
	69.28	16.2			14.06	8.7	
				region 3	0.30	38.3	2.75
					2.48	52.2	
					14.17	9.5	
				bulk water	0.27	36.2	2.88
					2.33	53.0	
					14.30	10.8	

strained environment due to simultaneous formation of two hydrogen bonds with two surfactant headgroups. Such a strained geometry of BW2 type water leads to faster relaxation of the corresponding correlation function. The decay curves show the presence of slow components at long times. Such slow long time decay cannot be described by a single exponential law. We have fitted the curves to multiexponentials, and the parameters for best fits along with the amplitude-weighted average time constants, $\langle\tau_c\rangle$, are listed in Table 1. The presence of a long time component (∼70 ps) for both types of water can be seen. The $\langle\tau_c\rangle$ value has been found to be about 30% shorter for BW2 type water molecules.

The relaxation of the $C_{WW}(t)$ decay curves for water molecules present in the three regions at the interface show interesting behavior. It is clear from Figure 2 that the relaxation of WW hydrogen bonds in region 1 is much slower than that for the other two regions and for pure bulk water. Again, such slow relaxation for region 1 water molecules arises due to their strong interaction with the surfactant headgroups. To verify this, we have calculated the average WW hydrogen bond energies for the three regions. These are found to be −3.6 kcal/mol for region 1, −3.7 kcal/mol for region 2, and −3.8 kcal/mol for region 3 water molecules. The corresponding value for pure bulk TIP3P water is around −4 kcal/mol. Our calculation reveals that the WW hydrogen bonds in all of the regions are marginally weaker than those in pure bulk water. However, as already discussed, water in region 1 can form much stronger hydrogen bonds with the surfactant headgroups. This more than compensates for the weaker WW hydrogen bonds in this region, as a significant fraction of these bonds would be disrupted and replaced by stronger SW hydrogen bonds with surfactant headgroups. The presence of such bound water eventually leads to slower dynamics of the water molecules in region 1, as compared to pure bulk water, as shown in Figure 2. The hydrogen bond energies of water in regions 2 and 3 have been found to be slightly higher than that for bulk water. As a result, the structural relaxation of the WW hydrogen bonds in these regions occurs relatively faster than that in pure bulk water. As the distance from the surfactant headgroups increases, the behavior of water molecules gradually approaches that of bulk water, which is evident from near identical relaxation behavior of WW hydrogen bonds in region 3 and that in pure bulk water. Such distance-dependent dynamics of WW hydrogen bonds has been observed earlier at water/organic liquid[12] and metal/water[53] interfaces. We have again fitted the $C_{WW}(t)$ decay curves to multiexponentials and listed the parameters for best fits and the average time constants, $\langle\tau_c\rangle$, in Table 1. It can be noted that the $\langle\tau_c\rangle$ values for WW hydrogen bonds are much shorter than those for the SW hydrogen bonds. Besides, due to the presence of bound water molecules in region 1, the average structural relaxation time of the WW hydrogen bonds in this region is about twice longer than the other regions and bulk water. The relaxation pattern of the WW hydrogen bonds in the three regions agrees nicely with the differential translational and reorientational dynamics of water in those regions, as reported earlier.[33]

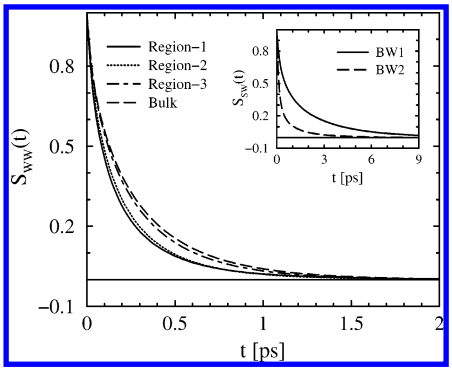

Figure 3. Continuous hydrogen bond time correlation function, $S_{WW}(t)$, for the hydrogen bonds formed between the water molecules in three regions of the aqueous layer as well as that for pure bulk TIP3P water. The definitions of the regions are the same as those in Figure 2. The inset shows the corresponding function, $S_{SW}(t)$, for BW1 and BW2 types of water molecules present in the first hydration layer (region 1).

In Figure 3, we display the relaxation of the continuous hydrogen bond correlation function, $S(t)$, for both WW and SW hydrogen bonds by averaging over different time origins. For comparison, the corresponding relaxation behavior for pure bulk TIP3P water is also included in the plot. Once again, the function $S_{SW}(t)$ is separately calculated for BW1 and BW2 types of water molecules, which are shown in the inset. In all cases, a rapid initial decay in the correlation function arising primarily due to the fast librational and vibrational motions of the hydrogen bonded sites have been noticed. We observe that the relaxation of the function for SW hydrogen bonds, $S_{SW}(t)$, is significantly slower than the corresponding function for WW hydrogen bonds, $S_{WW}(t)$. It is further noticed that the relaxation of $S_{SW}(t)$ is faster for the hydrogen bonds formed by BW2 type water molecules as compared to that formed by BW1 type. This is in accordance with the relaxation behavior of $C_{SW}(t)$, as observed earlier (Figure 2), and indicates relatively shorter lifetimes of SW hydrogen bonds formed by BW2 type water. This once again is due to the strained bonding environment associated with a BW2 water molecule. This leads to a shorter average lifetime of any one of the two SW hydrogen bonds that a BW2 water forms with two surfactant headgroups compared to the hydrogen bond formed by a BW1 water molecule. To obtain an estimate of the lifetimes of the SW hydrogen bonds, we have fitted the corresponding decay curves to a sum of two exponentials, and the parameters are listed in Table 2. The calculated $\langle\tau_s\rangle$ value for SW hydrogen bonds formed by BW1 water is found to be more than 3 times longer than the corresponding value for BW2 type water.

The relaxation of $S_{WW}(t)$ decay curves for the hydrogen bonds among water molecules present in the three regions at the interface again shows interesting behavior. At first, we note that all of the three decay curves relax faster than pure bulk water. This is particularly true for water in regions 1 and 2. The

TABLE 2: Multiexponential Fitting Parameters for the Surfactant−Water (SW), $S_{SW}(t)$, and Water−Water (WW), $S_{WW}(t)$, Continuous Hydrogen Bond Time Correlation Functions (Corresponding Parameters for Bulk TIP3P Water Are Also Listed for Comparison; $\langle\tau_s\rangle$ is the Average Time Constant)

surfactant−water (SW)				water−water (WW)			
type	time constant (ps)	amplitude (%)	$\langle\tau_s\rangle$ (ps)	region	time constant (ps)	amplitude (%)	$\langle\tau_s\rangle$ (ps)
BW1	0.28	48.0	1.45	region 1	0.05	48.6	0.17
	2.53	52.0			0.29	51.4	
BW2	0.14	74.8	0.41	region 2	0.05	40.3	0.18
	1.23	25.2			0.27	59.7	
				region 3	0.05	32.4	0.23
					0.32	67.6	
				bulk water	0.06	32.0	0.27
					0.37	68.0	

differences in WW hydrogen bond energy in the three regions may provide insight into such differential relaxation behavior. As defined in eq 1, the function $S(t)$ in general does not allow any reformation event and thus primarily reveal the dynamics of hydrogen bond breaking. Therefore, weaker hydrogen bonds should break faster and hence have shorter lifetimes. As discussed earlier, the strength of a WW hydrogen bond varies in the following order: region 1 < region 2 < region 3 < bulk water. Thus, the relaxation of $S_{WW}(t)$ decay curves seems to agree with this trend. We have again fitted these curves to multiexponentials, and the data are listed in Table 2. As expected, the results show that the average time constants, $\langle\tau_s\rangle$, for WW hydrogen bonds are much shorter than that for the SW hydrogen bonds. We find that the $\langle\tau_s\rangle$ values for WW hydrogen bonds in the three regions are approximately 15−40% shorter than that obtained for pure bulk water. It may be noted that the calculated $\langle\tau_s\rangle$ value of 0.27 ps for WW hydrogen bonds in pure bulk TIP3P water is closer to the lower end of the experimental values of the characteristic hydrogen bond time constant, which vary between 0.3 and 0.7 ps.[54]

3.3. Diffusion and Hydrogen Bond Dynamics. It is well-known that the dynamics of hydrogen bonds between two molecules is strongly coupled with the diffusion of the molecules.[4,5,9,55] When a hydrogen bond between two molecules is broken, they may remain in close contact for a while before either the said bond is reformed or the two participating molecules diffuse away from each other. Faster diffusion will result in faster hydrogen bond relaxation and vice versa. Luzar and Chandler[4] demonstrated that such coupling is the physical origin of the nonexponential relaxation of the hydrogen bond time correlation functions. To eliminate the contribution arising from the diffusion of hydration layer water molecules, we calculate the time correlation function[4,5,9,53,55]

$$N(t) = \frac{\langle h(0)(1 - h(t))H'(t)\rangle}{\langle h\rangle} \tag{3}$$

for both WW hydrogen bonds in the three interfacial regions and SW hydrogen bonds between the surfactant headgroups and the first hydration layer (i.e., region 1) water molecules. The variable $H'(t)$ is unity if the tagged pair of sites is closer than a cutoff distance, R_H (3.5 Å for both SW and WW hydrogen bonds) at time t, and zero otherwise. Thus, a nonzero value for $N(t)$ indicates that the tagged pair of sites are no longer hydrogen bonded but remain in the vicinity of each other (i.e., within R_H). A value of zero suggests that the two sites are either in the bonded state or separated by a distance larger than R_H. Thus, $N(t)$ describes the time-dependent probability that a particular hydrogen bond between a pair of sites is broken at time t, but the two sites have not diffused away and remain as nearest neighbors. The relaxation of $N(t)$ can occur due to reformation of the broken hydrogen bonds or due to diffusion of the two sites.[4]

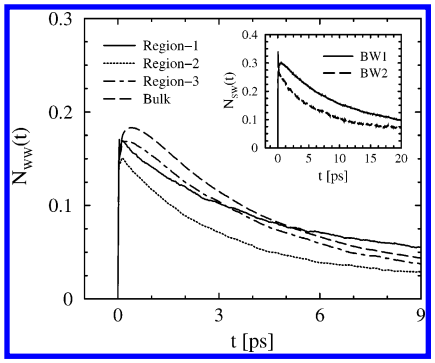

Figure 4. Time-dependent probability that a water−water (WW) hydrogen bond is broken but the two water molecules remain as nearest neighbors. The results obtained for water in three regions of the aqueous layer as well as that for pure bulk TIP3P water are displayed. The definitions of the regions are the same as those in Figure 2. The inset shows the corresponding probability function for BW1 and BW2 types of water molecules present in the first hydration layer (region 1).

In Figure 4, we display the relaxation of $N_{WW}(t)$ for the hydrogen bonds formed between the water molecules in the three regions. For comparison, we have also displayed the corresponding function for pure bulk TIP3P water. The inset shows the relaxation of $N_{SW}(t)$ for the SW hydrogen bonds formed separately by BW1 and BW2 types of water present in region 1. We observe that the relaxation of the function $N_{SW}(t)$ for both types of water molecules is much slower than the corresponding function for WW hydrogen bonds in the three regions. This is a signature of enhanced rigidity of the first hydration layer (region 1). Besides, we notice that the relaxation of $N_{SW}(t)$ is faster for hydrogen bonds between surfactant headgroups and BW2 type water. This is in accordance with the relaxation pattern observed for the SW hydrogen bond TCFs (Figures 2 and 3). A differential relaxation behavior is also observed for $N_{WW}(t)$ for water molecules present in the three regions which agrees well with the structural relaxation of the WW hydrogen bonds in these regions. For example, the slowly decaying tail for region 1 water molecules is in accordance with slow relaxation of these hydrogen bonds (Figure 2), which again indicates higher rigidity of water molecules in this region that are in direct contact with the surfactant headgroups. Similarly, the faster relaxation of $N_{WW}(t)$ for water molecules in regions 2 and 3 agrees too with the relaxation of WW hydrogen bonds in these regions.

3.4. Kinetics of Hydrogen Bond Breaking and Formation. We have further investigated the kinetics of breaking and reformation of WW and SW hydrogen bonds using the simple model proposed by Luzar and Chandler,[4,5] which is defined as

$$\mathrm{B} \rightleftharpoons \mathrm{QF} \tag{4}$$

Here, B denotes the bound state where two sites are hydrogen bonded to each other and QF is the quasi-free state, where the hydrogen bond is broken, but the two sites remain as nearest neighbors (i.e., within distance R_H). As per the definitions, the probabilities $C(t)$ and $N(t)$ correspond to local populations of states B and QF, respectively, which can interconvert according to eq 4. Following this model, we attempt here to connect the microscopic description of WW and SW hydrogen bond dynamics and phenomenological reaction kinetics of their

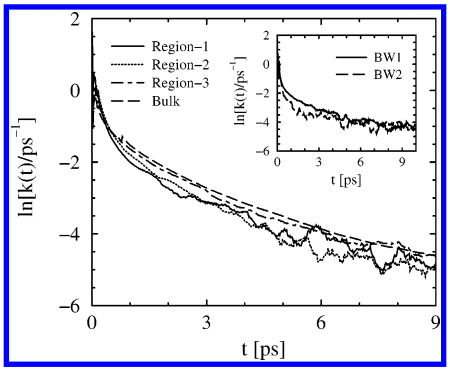

Figure 5. Water−water (WW) hydrogen bond reactive flux, $k(t)$ (semilog plot), for the breaking and reformation of hydrogen bonds in three regions of the aqueous layer as well as that for pure bulk TIP3P water. The definitions of the regions are the same as those in Figure 2. The inset shows the corresponding function for BW1 and BW2 types of water molecules present in the first hydration layer (region 1).

breaking and reformation. If k_1 and k_2 are the forward (breaking) and backward (reformation) rate constants, then a simple rate equation for the "reactive flux" can be written as

$$k(t) = -\frac{dC(t)}{dt} = k_1 C(t) - k_2 N(t) \qquad (5)$$

The relaxation of $k(t)$ to equilibrium occurs by transitions from reactants to products, that is, from state B to state QF (eq 4).

We have calculated $k(t)$ from the derivative of the simulated results of intermittent hydrogen bond TCF, $C(t)$, for both WW hydrogen bonds in the three interfacial regions as well as the SW hydrogen bonds. The results are displayed in Figure 5. For comparison, the result for pure bulk TIP3P water is also included in the figure. Besides, the calculations for SW hydrogen bonds are again carried out separately for the BW1 and BW2 types of water molecules, as shown in the inset of the figure. At short times (<0.5 ps), $k(t)$ relaxes fast for both WW and SW hydrogen bonds. This is the transient period,[4] and the sharp relaxation within this time scale arises due to fast librational and vibrational motions involving the hydrogen bonded sites. It is apparent from the figure that the function $k(t)$ decays quite monotonically for the WW hydrogen bonds in different regions of the interfacial aqueous layer. This is in contrast to the corresponding function for the SW hydrogen bonds, which although fluctuating attains plateau values reasonably quickly. This agrees well with the relaxation of WW and SW hydrogen bond TCFs as discussed earlier (Figures 2 and 4). Because of the stronger hydrogen bonds between the water in the first hydration layer (region 1) and the surfactant headgroups and the consequent slow diffusion[33] and rigid nature of water in region 1, the bond breaking and reformation equilibrium (eq 4) establishes quickly for SW hydrogen bonds. We have used the least-squares fit approach[9,52,53] for $t > 0.5$ ps to obtain the forward and backward rate constants (k_1 and k_2) that best satisfy eq 5 for all of the cases. These are listed in Table 3. The inverse of the forward rate constant ($1/k_1$), which corresponds to the average hydrogen bond lifetime, is also included in the table. It may be noted that the values of $1/k_1$ are larger than the respective $\langle\tau_s\rangle$ values of the hydrogen bonds, as obtained from the correlation function, $S(t)$ (Table 2). This is expected, as $S(t)$ primarily provides information about the dynamics of hydrogen bond breaking due to fast librational and vibrational motions, while the quantity $1/k_1$ additionally includes contributions from slower diffusional motion of water molecules.[52,53] It may be noted that the macroscopic rate law (eq 5) cannot resolve short time transient behavior and is applicable on a coarse-grained time scale. On the other hand, the correlation functions, as shown in Figures 2 and 3, can provide valuable information on different time scales associated with the dynamics, as shown in Tables 1 and 2.

TABLE 3: Forward (k_1) and Backward (k_2) Rate Constants for Surfactant−Water (SW) and Water−Water (WW) Hydrogen Bond Breaking and the Average Hydrogen Bond Lifetimes ($1/k_1$) as Obtained from a Least-Squares Fit of eq 5 (Corresponding Parameters for Bulk TIP3P Water Are Also Listed for Comparison)

surfactant-water (SW)				water−water (WW)			
type	k_1 (ps^{-1})	k_2 (ps^{-1})	$1/k_1$ (ps)	region	k_1 (ps^{-1})	k_2 (ps^{-1})	$1/k_1$ (ps)
BW1	0.52	0.48	1.92	region 1	0.88	1.30	1.13
BW2	0.71	1.09	1.41	region 2	1.16	1.84	0.86
				region 3	0.84	1.03	1.19
				bulk water	0.88	1.18	1.13

4. Conclusions

In this article, we have carried out an extensive atomistic MD simulation to study the hydrogen bond lifetime dynamics in the hydration layer of monolayers of an anionic surfactant, sodium salt of aerosol-OT or AOT adsorbed at the air/water interface with a surface coverage corresponding to that at the cmc. In particular, we have studied the lifetime dynamics of both surfactant−water (SW) and water−water (WW) hydrogen bonds at the interface. The SW hydrogen bond dynamics is investigated for two types of water molecules present at the interface, BW1 and BW2, depending on whether a water molecule forms one hydrogen bond with a surfactant headgroup or two hydrogen bonds with two different headgroups. The WW hydrogen bond dynamics is studied for water present in different hydration layers or regions by varying distances from the surfactant headgroups.

Our calculations reveal several interesting results. First of all, we find that the water present in the first hydration layer (region 1) forms strong hydrogen bonds with the surfactant headgroups. This leads to slower relaxation of SW hydrogen bond time correlation functions as compared to WW hydrogen bonds in both interfacial and pure bulk water. We have noticed that, due to geometrical constraints around BW2 water molecules, they form relatively weaker SW hydrogen bonds with shorter lifetimes than the BW1 water molecules. Equally interestingly, significant differences in the dynamical behavior of the WW hydrogen bonds have been noticed in different hydration layers or regions at the interface. It is observed that the WW hydrogen bonds in regions 2 and 3 of the aqueous layer are weaker than those in bulk. This results in faster structural relaxation of WW hydrogen bonds in these regions. Adopting the simple model as proposed by Luzar and Chandler,[4,5] we have studied the kinetics of breaking and reformation of both SW and WW hydrogen bonds. We have shown that, due to the higher strength of SW hydrogen bonds and the rigidity of the first hydration layer or region 1, the bond breaking and reformation equilibrium (eq 4) establishes quickly for SW hydrogen bonds. To the best of our knowledge, this is the first report where the lifetime dynamics of SW and WW hydrogen bonds in the hydration layer of a surfactant monolayer adsorbed at the air/water interface have been atomistically studied.

Finally, it may be noted that a change of the surfactant concentration at the interface can influence the dynamics of hydrogen bonds. However, this needs to be verified further. Currently, we are also investigating the hydrogen bond lifetime dynamics at the interface of monolayers containing a mixture of anionic and nonionic surfactant molecules.

Acknowledgment. This work was supported in part by generous grants from the Council of Scientific and Industrial Research (CSIR), Department of Science and Technology (DST), and the Department of Biotechnology (DBT).

References and Notes

(1) Eisenberg, D.; Kauzmann, W. *The Structure and Properties of Water*; Oxford University Press: New York, 1969.
(2) Teixeira, J. *J. Phys. IV* **1993**, *3*, 162.
(3) Stillinger, F. H. *Science* **1980**, *209*, 451; *Adv. Chem. Phys.* **1975**, *31*, 1.
(4) Luzar, A.; Chandler, D. *Nature (London)* **1996**, *397*, 55; *Phys. Rev. Lett.* **1996**, *76*, 928.
(5) Luzar, A. *J. Chem. Phys.* **2000**, *113*, 10663; *Chem. Phys.* **2000**, *258*, 267.
(6) Chen, S. H.; Teixeira, J. *Adv. Chem. Phys.* **1986**, *64*, 1. Dore J. C., Teixeira, J., Eds.; *Hydrogen-Bonded Liquids*; Kluwer Academic: Dordrecht, The Netherlands, 1991.
(7) Blumberg, R. L.; Stanley, H. E. *J. Chem. Phys.* **1984**, *80*, 5230. Sciortino, F.; Poole, P. H.; Stanley, H. E.; Havlin, S. *Phys. Rev. Lett.* **1990**, *64*, 1686.
(8) Ohmine, I.; Tanaka, H. *Chem. Rev.* **1993**, *93*, 2545. Ohmine, I.; Saito, S. *Acc. Chem. Res.* **1999**, *32*, 741.
(9) Xu, H.; Stern, H. A.; Berne, B. J. *J. Phys. Chem. B* **2002**, *106*, 2054.
(10) Chandra, A. *Phys. Rev. Lett.* **2000**, *85*, 768. Chowdhuri, S.; Chandra, A. *Phys. Rev. E* **2002**, *66*, 041203. Chowdhuri, S.; Chandra, A. *J. Phys. Chem. B* **2006**, *110*, 9674.
(11) Liu, P.; Harder, E.; Berne, B. J. *J. Phys. Chem. B* **2005**, *109*, 2949.
(12) Benjamin, I. *J. Phys. Chem. B* **2005**, *109*, 13711.
(13) Balasubramanian, S.; Pal, S.; Bagchi, B. *Phys. Rev. Lett.* **2002**, *89*, 115505.
(14) Pal, S.; Balasubramanian, S.; Bagchi, B. *J. Phys. Chem. B* **2003**, *107*, 5194.
(15) Pal, S.; Balasubramanian, S.; Bagchi, B. *Phys. Rev. E* **2003**, *67*, 061502.
(16) Bruce, C. D.; Senapati, S.; Berkowitz, M. L.; Perera, L.; Forbes, M. D. E. *J. Phys. Chem. B* **2002**, *106*, 10902.
(17) Faeder, J.; Ladanyi, B. M. *J. Phys. Chem. B* **2000**, *104*, 1033.
(18) Bagchi, B. *Chem. Rev.* **2005**, *105*, 3197.
(19) Tarek, M.; Tobias, D. J. *Biophys. J.* **2000**, *79*, 3244. Tarek, M.; Tobias, D. J. *Phys. Rev. Lett.* **2002**, *88*, 138101.
(20) Bagchi, B. *Annu. Rep. Prog. Chem., Sect. C: Phys. Chem.* **2003**, *99*, 127. Nandi, N.; Bhattacharyya, K.; Bagchi, B. *Chem. Rev.* **2000**, *100*, 2013. Bhattacharyya, K.; Bagchi, B. *J. Phys. Chem. A* **2000**, *104*, 10603.
(21) Cheng, Y. K.; Rossky, P. J. *Nature (London)* **1998**, *392*, 696.
(22) Jordinades, X. J.; Lang, M. J.; Song, X.; Fleming, G. R. *J. Phys. Chem. B* **1999**, *103*, 7995.
(23) Tarek, M.; Tobias, D. J.; Klein, M. L. *J. Phys. Chem.* **1995**, *99*, 1393.
(24) Wijmans, C. M.; Linse, P. *J. Phys. Chem.* **1996**, *100*, 12583.
(25) Kuhn, H.; Rehage, H. *J. Phys. Chem. B* **1999**, *103*, 8493.
(26) Kuhn, H.; Rehage, H. *Phys. Chem. Chem. Phys.* **2000**, *2*, 1023.
(27) Kuhn, H.; Rehage, H. *Colloid Polym. Sci.* **2000**, *278*, 114.
(28) Dominguez, H. *J. Phys. Chem. B* **2002**, *106*, 5915.
(29) Stone, M. T.; da Rocha, S. R. P.; Rossky, P. J.; Johnston, K. P. *J. Phys. Chem. B* **2003**, *107*, 10185.
(30) Rekvig, L.; Hafskjold, B.; Smit, B. *J. Chem. Phys.* **2004**, *120*, 4897.
(31) Rekvig, L.; Hafskjold, B.; Smit, B. *Phys. Rev. Lett.* **2004**, *92*, 116101.
(32) Bandyopadhyay, S.; Chanda, J. *Langmuir* **2003**, *19*, 10443.
(33) Chanda, J.; Chakraborty, S.; Bandyopadhyay, S. *J. Phys. Chem. B* **2005**, *109*, 471.
(34) Chanda, J.; Bandyopadhyay, S. *J. Chem. Theor. Comput.* **2005**, *1*, 963.
(35) Zimdars, D.; Eisenthal, K. B. *J. Phys. Chem. A* **1999**, *103*, 10567. Benderskii, A. V.; Eisenthal, K. B. *J. Phys. Chem. B* **2000**, *104*, 11723. Benderskii, A. V.; Eisenthal, K. B. *J. Phys. Chem. A* **2002**, *106*, 7482.
(36) Pantano, D. A.; Sonoda, M. T.; Skaf, M. S.; Laria, D. *J. Phys. Chem. B* **2005**, *109*, 7365.
(37) Li, Z. X.; Lu, J. R.; Thomas, R. K.; Penfold, J. *J. Phys. Chem. B* **1997**, *101*, 1615.
(38) Martyna, G. J.; Tuckerman, M. E.; Tobias, D. J.; Klein, M. L. *Mol. Phys.* **1996**, *87*, 1117.
(39) Tuckerman, M. E.; Yarne, D. A.; Samuelson, S. O.; Hughs, A. L.; Martyna, G. J. *Comput. Phys. Commun.* **2000**, *128*, 333.
(40) Darden, T.; York, D.; Pedersen, L. *J. Chem. Phys.* **1993**, *98*, 10089.
(41) Procacci, P.; Darden, T.; Marchi, M. *J. Phys. Chem.* **1996**, *100*, 10464.
(42) Procacci, P.; Marchi, M.; Martyna, G. J. *J. Chem. Phys.* **1998**, *108*, 8799.
(43) Allen, M. P.; Tildesley, D. J. *Computer Simulation of Liquids*; Clarendon: Oxford, U.K., 1987.
(44) Schlenkrich, M.; Brickmann, J.; MacKerell, A. D.; Karplus, M. *Empirical Potential Energy Function for Phospholipids: Criteria for Parameter Optimization and Applications*, in *'Biological Membranes: A Molecular Perspective from Computation and Experiment*; Birkhauser: Boston, MA, 1996.
(45) Jorgensen, W. L.; Chandrasekhar, J.; Madura, J. D.; Impey, R. W.; Klein, M. L. *J. Chem. Phys.* **1983**, *79*, 926.
(46) Mezei, M.; Beveridge, D. L. *J. Chem. Phys.* **1981**, *74*, 622.
(47) Luzar, A.; Chandler, D. *J. Chem. Phys.* **1993**, *98*, 8160.
(48) Rahman, A.; Stillinger, F. H. *J. Chem. Phys.* **1971**, *55*, 3336.
(49) Stillinger, F. H.; Rahman, A. *J. Chem. Phys.* **1974**, *60*, 1545.
(50) Rapaport, D. C. *Mol. Phys.* **1983**, *50*, 1151.
(51) Benjamin, I. *J. Chem. Phys.* **1999**, *110*, 8070.
(52) Chanda, J.; Chakraborty, S.; Bandyopadhyay, S. *J. Phys. Chem. B* **2006**, *110*, 3791.
(53) Paul, S.; Chandra, A. *Chem. Phys. Lett.* **2004**, *386*, 218.
(54) Neinhuys, H. K.; Woutersen, S.; van Santen, R. A.; Bakker, H. J. *J. Chem. Phys.* **1999**, *111*, 1494. Woutersen, S.; Emmerichs, U.; Bakker, H. J. *Science* **1997**, *278*, 658. Kropman, M. F.; Bakker, H. J. *Science* **2001**, *201*, 2118. Kropman, M. F.; Bakker, H. J. *J. Chem. Phys.* **2001**, *115*, 8942.
(55) Xu, H.; Berne, B. J. *J. Phys. Chem. B* **2001**, *105*, 11929.